

EXPERIMENTAL ANALYSIS OF INTERFACIAL PROPERTIES OF SPHERE OBLIQUE IMPACT WITH INITIAL SPIN

QING-PENG WANG, ZHEN-FENG WANG

*Henan Agricultural University, College of Mechanical and Electrical Engineering, Zhengzhou, China, and
Henan Agricultural University, Henan Provincial Cold Chain Information and Equipment Laboratory
for Logistics of Agricultural Products, Zhengzhou, China
e-mail: welcomewqp@163.com; zhenfengking@qq.com*

HENG WANG, DE-FENG LI, XIAN-KUN GAO

*Henan Agricultural University, College of Mechanical and Electrical Engineering, Zhengzhou, China
e-mail: 45108868@qq.com; 13140027027@163.com; gaoxiankun78@163.com*

GUANG-YIN XU

*Henan Agricultural University, College of Mechanical and Electrical Engineering, Zhengzhou, China, and
Henan Agricultural University, Henan Provincial Cold Chain Information and Equipment Laboratory
for Logistics of Agricultural Products, Zhengzhou, China
e-mail: xgy4175@126.com*

Experiments of a sphere oblique impact with and without an initial spin have been carried out to obtain properties of the impact interface. The contact surface is recorded with a piece of thin carbon paper. The interfacial parameters measured are expressed as axis length, contact area and slip ratio. It is found that for the impact between steels the forward spin can make geometrical sizes of the contact surface increase compared with the case of no initial spin, however, just the reverse for the backward spin. The effect of the initial spin becomes more apparent for the impact with a rubber cushion. Whether the initial spin promotes or hinders the sphere sliding depends on the parameters of tangential velocity and force at the interface.

Keywords: sphere, spin, oblique impact, contact surface, slip ratio

1. Introduction

The impact of a sphere with a flat surface is a common and fundamental event which is present in many granular handling processes of mechanical, mineral, agricultural, chemical and pharmaceutical industries (Moreno *et al.*, 2003; Mueller *et al.*, 2011; Cross, 2019; Fu *et al.*, 2020; Ye *et al.*, 2021). It has significant effects on the state of motion of the collision system and the integrity of granular appearance.

At present, the existing methods to study the sphere impact can be mainly divided into three classes: theoretical analysis, numerical simulation and experimental test. Firstly, in theory, there are two kinds of models: discontinuous and continuous descriptions. The first kind is based on a series of phenomenological parameters of the coefficients of restitution (COR) and friction (COF). The pioneering works of Newton concentrated on investigating the notion of COR defined the ratio of post-impact to pre-impact velocities taken normal to the impact plane (Dong and Moys, 2006). Many models have been developed by these parameters to describe motion states of sticking, sliding and rolling during impact. Representative examples are Brach (1984), Walton (1993), Foerster *et al.* (1994), Lorenz *et al.* (1997), Mueller *et al.* (2011), Doménech-Carbó (2021). The second kind is based on the concepts of normal contact force and tangential slip inspired

by the theories developed by Hertz and Mindlin (Maw *et al.*, 1977; Thornton and Ning, 1998; Stronge *et al.*, 2001; Müller and Pöschel, 2012; Chehaibi *et al.*, 2019). Hertz presented a linear elastic relationship between a static contact force and normal displacement, and Mindlin used the loading history of normal and tangential forces to formulate the current tangential force, the interfacial states changed from sticking to sliding can be described. Representative models are Maw *et al.* (1977), Thornton and Ning (1998), Stronge *et al.* (2001), Müller and Pöschel (2012).

Generally speaking, the impact behavior can be identified by two kinds of models, and the corresponding parameters of the restitution coefficient and stiffness are consistent inherently, which are related with mechanical parameters, like elastic modulus E , Poisson's ratio ν , further, factors of surface energy, van der Waals force and electromagnetic force. The first kind of model has the advantages of simplicity and analytical character, the constant parameters obtained from motion states before and after impact can be used without considering nonlinear factors. Actually, it is reasonable under conditions of low-velocity impact without adhesion (Doménech-Carbó, 2021). Strictly, these parameters change with the impact angle, incoming velocity and other factors (Dong and Moys, 2006; Cross, 2019). The second kind of model can offer a deeper description of impact behavior at the interface, such as the contact force, contact area, energy dissipation. In addition, the effects of geometrical, material and interfacial nonlinear characters can be included in this kind of model. However, the involved parameters of the elastic modulus E , Poisson's ratio ν and COF have to be obtained from experiments independent of the impact event. It is evident that some empirical information needs to be known *a priori* (Doménech-Carbó, 2021).

Several studies have been performed on the oblique impact using numerical methods, such as discrete element method (DEM) (Moreno *et al.*, 2003; Di Renzo and Di Maio, 2004; Gao *et al.*, 2019) and finite element method (FEM) (Wu *et al.*, 2003; Aryaei *et al.*, 2010; Hashemnia and Askari, 2019). In the modeling process, the simplest approach is that the individual particle is assumed as a rigid body, and the parameters of CORs and COF between the particles and particle-wall are kept constant (Di Renzo and Di Maio, 2004; Gao *et al.*, 2019). However, it might be inaccurate, because the contact bodies may deform, and the CORs vary with particle size, impact angle, initial spin, etc. during the impact (Wu *et al.*, 2003; Dong and Moys, 2006; Aryaei *et al.*, 2010; Hashemnia and Askari, 2019).

A number of researchers have investigated the sphere oblique impact experimentally (Foerster *et al.*, 1994; Lorenz *et al.*, 1997; Gorham and Kharaz, 2000; Kharaz *et al.*, 2001; Dong and Moys, 2006; Aryaei *et al.*, 2010; Mueller *et al.*, 2011; Komarnicki *et al.*, 2017; Cross, 2019; Hashemnia and Askari, 2019; Takizawa *et al.*, 2020). Foerster *et al.* (1994) proceeded an experiment of collision of a sphere without an initial spin, and modeled it in terms of three coefficients. Subsequently, Lorenz *et al.* (1997) reported the impact properties of small, nearly spherical particles. Gorham and Kharaz (2000) and Kharaz *et al.* (2001) measured velocities, angles and angular velocities before and after an impact of a 5 mm aluminum oxide sphere to a 26 mm thick soda lime glass, and a 25 mm aluminum alloy anvil using a digital camera with high precision. Of particular interest is the experimental study conducted by Dong and Moys (2006), who proceeded oblique impacts of a 44.5 mm steel sphere dropped freely on a steel flat surface with and without an initial spin. They concluded that the forward spin promotes sliding of the sphere, but backward spin hinders sliding. Similarly, the effects of the ball size, impact velocity, initial spin, material, etc. on the impact properties were studied experimentally (Aryaei *et al.*, 2010; Mueller *et al.*, 2011; Cross, 2019; Hashemnia and Askari, 2019). Mueller *et al.* (2011) observed that the normal COR is independent of the impact angle and impact velocity, and the tangential COR shows a minimum at an impact angle between 20° and 30°. Takizawa *et al.* (2020) developed a novel apparatus of a granular impact experiment by which the incident angle of projectile and

the inclination angle of the target layer could be independently varied. They found that the COR is independent of the inclination angle of the target surface and exponentially increases with the incident angle. Komarnicki *et al.* (2017) measured the contact area between the tested fruit and fixed material for different drop heights to assess bruise resistance.

With regard to the oblique impact of a sphere with a flat surface, the COR obtained from the velocities before and after impact has always been used to study the variation of the sphere motion state by the majority of researchers. However, they always ignored the change of interfacial behavior during the impact, such as contact area, sphere slip. As a matter of fact, the contact area, which is an important center parameter, expands the research scale from one dimension to two dimensions, or from the macroscopic to microscopic scale. In addition, a problem remains how to quantitatively characterize the percentage of sphere slip at the interface. For these reasons, based on geometrical features of the impact interface, the calculation formulas of the contact area and the slip ratio are proposed. In this research, the effects of the initial spin, impact angle, cushion thickness and sphere material density on the parameters of geometrical size and slip ratio are analyzed through an experimental apparatus of a sphere with and without an initial spin obliquely impacting a flat surface.

2. Theory

A sphere with diameter of d_s falls freely from a height h_0 onto a flat surface inclined by α . The directions of forward and backward are defined according to the work of Dong and Moys (2006), as shown in Fig. 1a. If α is 0° , in other words, there is only a normal load at the impact interface, according to the contact theory initiated by Hertz, the contact surface is a regular circle. If the impact angle α is larger than 0° , both the normal and tangential loads simultaneously act on the impact interface, according to the slip theory developed by Mindlin the contact surface is not a regular circle, but has a shape close to an ellipse in Fig. 1b. In the process of an oblique impact, assuming that the normal and tangential components operate independently, the shape of the contact surface generated by the normal force is defined as a base circle. When there is a tangential force at the interface, the sphere will be in a state of micro-slip or slip. In one dimension scale, size of the major axis of the contact surface is larger than the minor axis or diameter of the base circle. Further, the area of the contact surface is larger than the base circle in the two dimension scale.

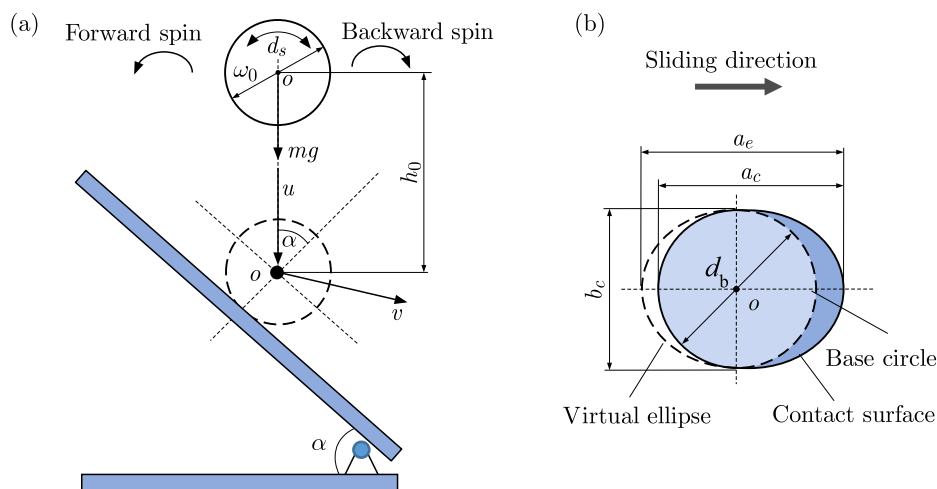


Fig. 1. (a) Oblique impact of a sphere with and without an initial spin and (b) its contact surface

Based on the above analysis, the slip ratio can be defined separately by the one dimension scale of length and two dimension scale of area, as

$$R_l = \frac{a_c - b_c}{b_c} \quad R_a = \frac{A_c - A_b}{A_b} \quad (2.1)$$

where a_c and b_c are lengths of the major and minor axis of the contact surface, respectively. A_c and A_b are the areas of the contact surface and base circle, respectively.

The contact surface consists of a base circle and a slip surface. The area of the base circle can be written as

$$A_b = \frac{\pi d_b^2}{4} \quad (2.2)$$

where d_b is the diameter of the base circle.

The slip area is half of the difference between the areas of the virtual ellipse and base circle, i.e.

$$A_s = \frac{A_e - A_b}{2} = \frac{\pi(a_e b_e - d_b^2)}{8} \quad (2.3)$$

where a_e and b_e are lengths of the major and minor axis corresponding to the virtual ellipse which is an envelope of the contact surface.

The total contact area is a sum of the areas of the base circle and the slip surface

$$A_c = A_b + A_s \quad (2.4)$$

Substituting Eqs. (2.2)-(2.4) into Eq. (2.1)₂, then

$$R_a = \frac{a_e b_e}{2d_b^2} - \frac{1}{2} \quad (2.5)$$

Assuming that there is no lateral slip during the oblique impact, i.e.

$$b_c = b_e = d_b \quad (2.6)$$

Equation (2.5) can be rewritten as

$$R_a = \frac{a_e}{2d_b} - \frac{1}{2} \quad (2.7)$$

There is a relation in the sliding direction

$$a_e = d_b + 2(a_c - d_b) \quad (2.8)$$

Substituting Eq. (2.8) into Eq. (2.7), thus

$$R_a = \frac{a_c - d_b}{d_b} \quad (2.9)$$

According to Eq. (2.6), Eq. (2.9) can be rewritten as

$$R_a = \frac{a_c - b_c}{b_c} \quad (2.10)$$

It can be seen from Eqs. (2.1)₁ and (2.10) that the results of the slip ratio calculated from the one and two dimension scales are uniform.

3. Test procedure

The experimental platform of a sphere obliquely impacting a flat surface has been constructed as shown in Fig. 2. It is mainly composed of four parts.

- (i) Control section of sphere motion. Firstly, regarding the sphere with an initial spin, a 5 mm wide paper band has been applied to wind around the sphere by a full turn. One end of the band is fixed to an electromagnetic inductor by a sticky tape, the other end is lightly glued onto the equator of sphere, so that the sphere can be dropped with the initial spin, rather than directly falling without it. For purpose of comparison, the sphere without the initial spin has been controlled by the electromagnetic inductor, once in which the current is removed by switching off electrical power, the sphere suspended at a certain height will fall freely onto the inclined steel plate.
- (ii) Rack section. A massive steel plate with a size of 500 mm×350 mm×10 mm has been designed to incline from 0° to 90° around the center of the bearing. The electromagnetic inductor is connected to the support bracket by a string.
- (iii) Measurement section of the characteristic parameters. A piece of printing paper (210 mm×150 mm×0.096 mm) is laid flat onto the steel plate, and then covers a piece of thin carbon paper (127 mm×90 mm×0.028 mm). The rubber cushions (500 mm×255 mm) with different thickness 1 mm-4 mm have been used to obtain a greater and clearer contact surface. In this way, the contact surface between the sphere and the plate can be printed onto the printing paper. The sizes of the major and minor axis are measured by a micrometer caliper, and then the contact area and the slip ratio are calculated by the proposed formulas. Besides, the normal impact force can also be obtained by a uniaxial accelerometer (CT1002L, 250 g) to compare with the theory models.
- (iv) Adjusting section of impact conditions. The drop height of the sphere from the impact position at the steel plate has been adjusted through a ruler, and the inclination angle of the steel plate by an angle gauge.

The contact area and the slip ratio have been calculated from the geometrical size of the impact surface obtained from the measurements, and then laws of its change at different impact cases can be analyzed.

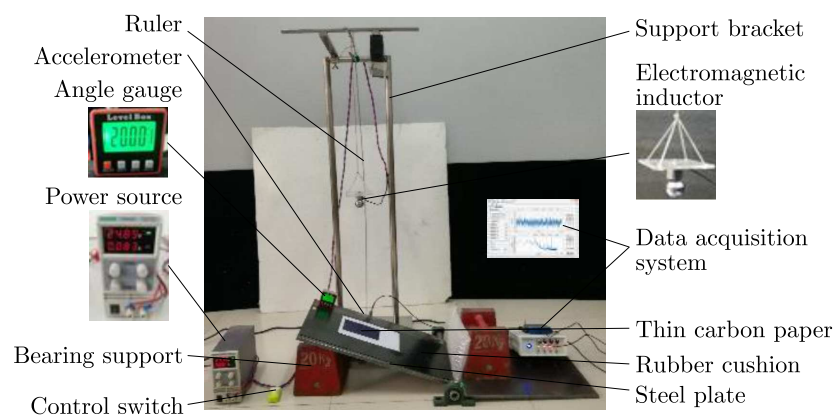


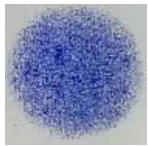
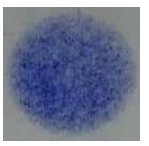
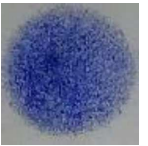
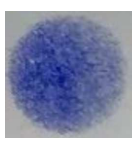
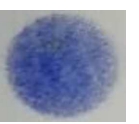
Fig. 2. Test device of the oblique impact

4. Experimental results

Using the test device of the oblique impact for the sphere with and without an initial spin, the effects of impact angle, cushion thickness and sphere material on the size of contact surface and

the slip ratio can be analyzed. For each case, the test has been repeated 10 times to ensure repeatability of the results, and then an average is taken. When a 30 mm diameter steel sphere impacts a steel plate on which a piece of rubber cushion with a thickness of 4 mm is laid flat, the contact surfaces at different impact angles are shown in Table 1.

Table 1. Contact surfaces at different impact angles

Impact angle	0°	10°	20°
Contact surface			
$a_c \times b_c$	10.473×10.437	10.196×9.918	10.088×9.807
Impact angle	30°	40°	50°
Contact surface			
$a_c \times b_c$	9.970×9.408	9.504×9.333	9.360×8.860
Impact angle	60°	70°	80°
Contact surface			
$a_c \times b_c$	9.091×8.247	8.747×7.082	8.482×5.540

Note: The unit of length of tex contact surface is mm

4.1. Effect of impact angle

A 30 mm steel sphere is dropped from a height of 400 mm onto a steel plate that is inclined from 0° to 80° at an increment of 10°. The results are shown in Fig. 3.

The sizes of the major axis of the contact surface are shown in Fig. 3a. When the impact angle α is smaller than about 30°, the normal component of the impact force is larger than the tangential component. The axis lengths for different motion modes all change slightly, and the average for the no pre-spin case is about 3.46 mm. By contrast, the average of the backward spin is 3.36 mm and decreases by 2.89%. An opposite trend is observed for the forward spin which is about 3.51 mm and increases by 1.45%. With the impact angle increasing, the axis lengths decrease nearly synchronously. When $\alpha > 60^\circ$, it presents some uncertain variations on the curves, which may be mainly due to deviations of the rotating speed and impacting position in each test. The sizes of minor axis shown in Fig. 3b are shorter than the major axis, but their laws of change are similar. The length ratio between the minor axis and major axis becomes smaller with the impact angle, that is to say, the contact surface becomes slimmer, as shown in Table 1.

The areas of the contact surface and the base circle against the impact angle are plotted in Fig. 3c. The area of the base circle is corresponding to the minor axis, and the contact surface is a combined result of the major and minor axis, so they have similar laws of change to the axis length. The forward spin can increase the contact area compared with the no initial spin, however, quite the contrary to the backward spin.

Figure 3d presents the slip ratios for different initial spins. When $\alpha < 30^\circ$, the normal component of the impact force plays a primary role, and the corresponding friction force is greater than the tangential component, so the sphere can not slide obviously. About the sphere spins, the direction of the driving force generated by the forward spin is the same as the tangential component of the gravity force, therefore, the sphere will slide at a smaller impact angle compared with the no initial spin case. It is opposite to the backward spin. When $\alpha > 30^\circ$, the slip ratios for the three cases keep nearly constant. After 60° of the target inclination, the tangential component of the impact force turns into a leading function, which makes the sphere slide more easily, and the slip ratio rapidly increase. Because the friction force for the forward spin is larger than the backward spin, it will make the sphere leave the plate firstly, and accordingly, the slip ratio will have a smaller value.

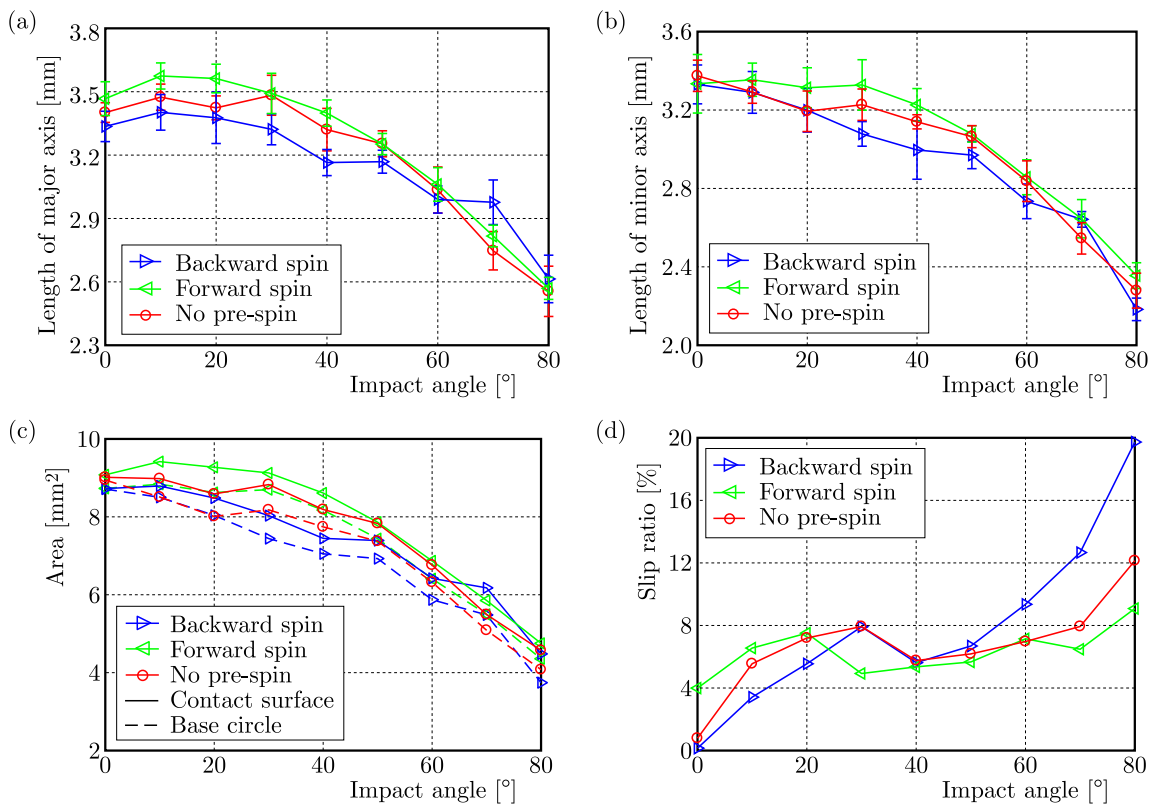


Fig. 3. Contact characteristic parameters of (a) major axis length, (b) minor axis length, (c) area and (d) slip ratio of the oblique impact at different impact angles

4.2. Effect of rubber cushion

A 30 mm diameter steel sphere falls from a height of 400 mm onto the rubber cushion with different thicknesses of 1 mm-4 mm (represented by the notation of t), which is laid flat onto an inclined steel plate. The geometrical sizes and the slip ratio are presented in Fig. 4.

It can be seen from Fig. 4a that the axis lengths of the contact surface in the cases of adding the cushion are greater than in the no cushion case. The increase rates of unit thickness for different cushion thicknesses of 1 mm-4 mm are separately 108.81%, 18.30%, 8.32% and 8.26%. From this, the increase rate of the major axis decreases with cushion thickness. The values of the forward spin are larger than the backward spin, and both of them are greater than in the no pre-spin case. The minor axis has a similar variation in Fig. 4b, the difference is that the results of the forward spin are slightly larger than or approximately equal to the backward spin.

The change of the areas is consistent with the axis length as shown in Fig. 4c. The increase rates of the contact area for unit thickness from 1 mm to 4 mm are separately 358.15%, 40.52%, 17.26% and 13.14%. In fact, the contact area is positively associated with dissipation of the applied energy during the impact. We know that more impact energy can be absorbed by adding a thicker cushion. However, the ability to absorb energy for unit thickness decreases with the increasing cushion thickness. It can be inferred that it has an optimum value of cushion thickness to absorb applied energy.

The slip ratios at different cushion thicknesses are all below 6% when $\alpha < 30^\circ$, and they increase slowly with cushion thickness. The result of the backward spin is close to the no pre-spin case, and both are greater than the forward spin. When $\alpha > 30^\circ$, the slip ratios for the three spin cases all increase gradually, and the results of the forward spin tend to the case of no pre-spin. At more oblique angles ($> 60^\circ$ here), the slip ratio at different impact cases increases sharply. However, these variations do not present some obvious law.

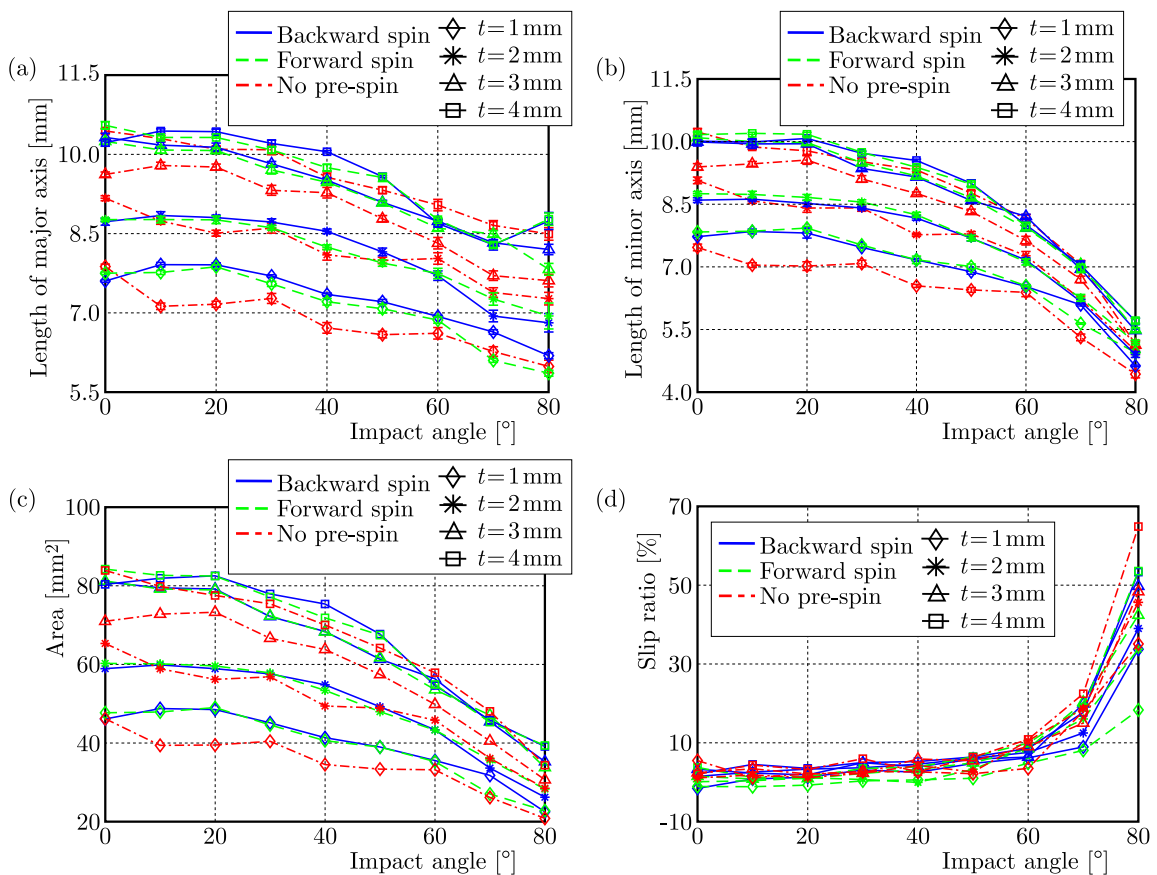


Fig. 4. Contact characteristic parameters of (a) major axis length, (b) minor axis length, (c) area and (d) slip ratio of oblique impact for different cushion thicknesses

4.3. Effect of sphere material

A 20 mm spheres made of different materials of steel, copper and aluminium are dropped from a height of 400 mm onto a rubber cushion with a thickness of 2 mm. The results are shown in Fig. 5.

The changes of geometrical sizes and slip ratios at different motion states are consistent with the above results. When $\alpha < 30^\circ$, the axis length of the copper sphere is a little greater than that of steel, and both are obviously greater than that of aluminium, see Figs. 5a and 5b. This is because densities of copper and steel are respectively 8.96 g/cm^3 and 7.93 g/cm^3 , which are

larger than density of aluminium of 2.70 g/cm^3 . The sizes of the contact surface for different materials clearly decrease with the impact angle. When $\alpha > 60^\circ$, the decrease rates of different materials all become small, and the changes for steel and copper are more noticeable than for aluminium. It is due to a greater tangential force for a heavier sphere, which can delay the decrease of the axis length and contact area. The slip ratios are shown in Fig. 5d, there is no obvious change law among different materials.

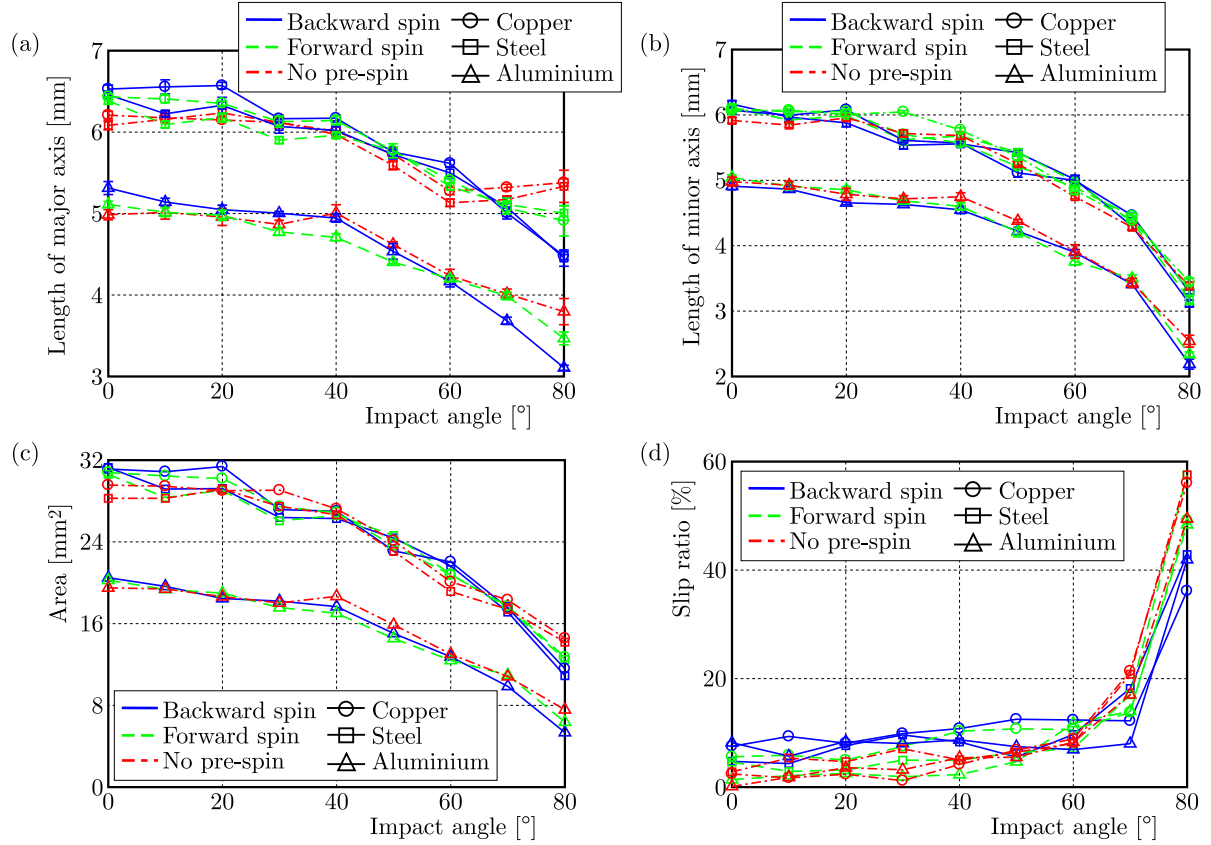


Fig. 5. Contact characteristic parameters of (a) major axis length, (b) minor axis length, (c) area and (d) slip ratio of the oblique impact for different contact materials

5. Discussion

The adhesion at the interface is very important for the change of the motion states after the impact, however, it has little effect on the contact area owing to the small adhesion force. For example, based on JKR model, the value is just 2.4 mN for a 20 mm steel sphere with its surface free energy being 50 mJ/m^2 . The two models of elastic and plastic loading without adhesion presented in work of Thornton and Ning (1998) can be applied to analyze the contact state at the impact interface

$$A_{c-e} = \pi R^3 \sqrt{\left(\frac{3F_{ic}}{4E\sqrt{R}}\right)^2} \quad A_{c-p} = \frac{F_{ic} - F_y}{\sigma_y} + \pi r_{c-y}^2 \quad (5.1)$$

where F_{ic} is the impact contact force obtained from the experiment, E is the effective elastic modulus, F_y and r_{c-y} are respectively the contact force and contact radius at yield, σ_y is the yield stress.

Because of the effects of printing paper and carbon paper, the contact areas obtained from the experiment are larger than the calculation results for the normal impact between the 20 mm steel sphere and the steel plate, as shown in Fig. 6. Taking the minimum and maximum of the contact area without the initial spin as reference points, the elastic and plastic results are respectively multiplied by 72 and 42. The results show that the impact interface should be in a mixed elastic-plastic state. In addition, the contact force and the contact area with the initial spin are greater than those without the initial spin.

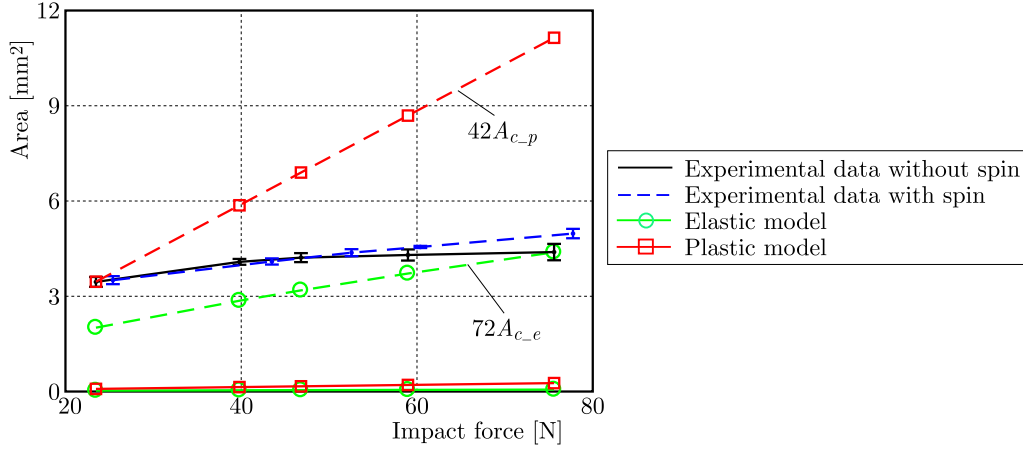


Fig. 6. Comparisons between impact contact models and experimental data for the normal impact of a steel sphere with a steel plate

Based on the above experimental results, the characteristic parameters at the impact interface can be analyzed to identify the variation of the sphere motion state, which may be sticking, sliding, rolling or their mixed compositions. The sphere adheres to the flat surface, and then it achieves a state of rolling after the impact due to the torque generated by the component of the contact force along the plate surface (Maw *et al.*, 1977). The rolling of the sphere can not be identified from the contact surface. Hence, the states of sticking and sliding at the interface will be discussed. The conditions of potential interfacial states at different initial spins are shown in Table 2.

Table 2. Conditions of potential interfacial states at different initial spins

Sphere motion state before impact	Interfacial state	Conditions
No spin $\omega = 0, v \sin \alpha > 0$	Sticking	$(r\omega + v \sin \alpha) > 0, F_t < \mu F_n $
	Sliding \downarrow	$(r\omega + v \sin \alpha) > 0, F_t \geq \mu F_n $
Forward spin $\omega > 0, v \sin \alpha > 0$	Sticking	$(r\omega + v \sin \alpha) > 0, F_t < \mu F_n $
	Sliding \downarrow	$(r\omega + v \sin \alpha) \gg 0, F_t \geq \mu F_n $
	Reverse sliding \uparrow	$(r\omega + v \sin \alpha) \gg 0, F_t < \mu F_n $
Backward spin $\omega < 0, v \sin \alpha > 0$	Sticking	$(r\omega + v \sin \alpha) < 0$ or $(r\omega + v \sin \alpha) > 0, F_t < \mu F_n $
	Sliding \uparrow	$(r\omega + v \sin \alpha) \ll 0, F_t \geq \mu F_n $
	Reverse sliding \downarrow	$(r\omega + v \sin \alpha) \ll 0, F_t < \mu F_n $

Note: \uparrow corresponds to the sliding direction of the sphere directed up to the slanted plane, and \downarrow directed down to the slanted plane

The geometrical parameters of the contact surface can be divided into three phases with the impact angle increasing: nearly flat, decrease and bifurcation. The slip ratio corresponds to the three phases: slow increase, flat and sharp increase.

(I) In the first phase, for the no initial spin case, the normal component of the impact force plays a dominating role when the impact angle is smaller than about 30° . The variation of different characteristic parameters is similar to the cosine curve, showing a nearly flat phase. Accordingly, the interfacial state is mainly sticking, and the slip ratio slightly increases when $|F_t| \geq \mu|F_n|$, which is comparable with the results presented in (Dong and Moys, 2006; Maw *et al.*, 1977).

With regard to the forward spin, the percentage of the downward pressure is greater than the upward one, and the normal component of the impact force further increases on the basis of the no initial spin situation. Hence, the sphere will produce a larger deformation and contact area. The backward spin has an opposite function. There is the same change trend for the normal coefficient of restitution in the work of Dong and Moys (2006), the values of it are respectively 0.9, 0.93 and 0.86 for the three cases of no initial spin, forward spin and backward spin, because a large restitution velocity always arises from a great impact force. Similar results can be found in (Wu *et al.*, 2003; Mueller *et al.*, 2011; Takizawa *et al.*, 2020).

However, it is not consistent with the impact between the sphere and rubber cushion, which shows that the results with different initial spins are approximately equal to or greater than in the no initial spin case. If the interfacial friction is large enough, the sphere can not roll on the rubber cushion, the normal parameters have little difference for the three cases, for example, during the impact between the 20 mm steel sphere and the 2 mm rubber cushion. Conversely, the sphere will continue to roll due to its own rotating inertia, which leads to further deforming of the rubber cushion. No matter the forward spin or backward spin, the corresponding geometrical parameters are greater than in the no initial spin case, for example, during the impact between the 30 mm steel sphere and the 1 mm rubber cushion.

Generally speaking, the initial spin promotes sliding of the sphere when the tangential force is greater than the interfacial friction, i.e. $|F_t| \geq \mu|F_n|$. On the contrary, it will hinder sliding, even slide reversely, when the sphere has enough rotational kinetic energy, however, which can not overcome the frictional resistance, i.e. $|F_t| < \mu|F_n|$ and $|r\omega + v \sin \alpha| \gg 0$. For example, in the oblique impact between the 30 mm steel sphere and the steel plate, the forward spin will promote sliding at lower impact angles, but the backward spin has an opposite function. Similar to the impact of copper and aluminium spheres in Fig. 5d, by contrast, for the impact between the 30 mm steel sphere and the rubber cushion both initial forward and backward spins can almost oppose sphere sliding due to a larger friction coefficient, see Fig. 4d. The above analyses are different from the viewpoint expressed by Dong *et al.* that the forward spin just promotes sliding, while the backward spin hinders sliding (Dong and Moys, 2006).

(II) In the middle phase, the normal component of the impact force decreases gradually with the impact angle, and the characteristic parameters of the contact surface decrease monotonically, called a decrease phase. Because of nearly synchronous variation of the major and minor axis of the contact surface, the slip ratio changes slightly, called a flat phase. The conditions of $(r\omega + v \sin \alpha) \ll 0$, $|F_t| \geq \mu|F_n|$ are matched for the backward spin which contributes to slide directed up to the slanted plane, quite reverse for the forward spin. It is consistent with the results of the impulse ratio defined as the ratio of the tangential impulse to the normal impulse presented in the work of Dong and Moys (2006), which are respectively 0.103, 0.09 and 0.11 for the three cases of no initial spin, forward spin and backward spin. Actually, a large impulse ratio corresponds to a great tangential force, which can make the sphere slide easily.

(III) In the final phase, the macro slip of the sphere can be occurred at the interface, which leads to a considerable difference between the major and minor axis, called a bifurcation phase. Correspondingly, the slip ratio is in the stage of a sharp increase. In fact, the experimental results of the oblique impact obtained by Dong and Moys (2006) just belong to the first two phases as the above mentioned. In this phase, the sphere can slide more easily at the interface, which will generate a long, narrow shape close to an ellipse. The effect of the initial spin is the

same as the analyses of the first two phases. However, a greater deviation exists in the change of the characteristic parameters because of uncertain factors of rotational speed, impact location, friction coefficient, etc.

6. Conclusions

A free fall apparatus has been used to determine interfacial parameters during a sphere oblique impact. The sphere can be released with and without an initial spin. The contact surface is recorded with a piece of thin carbon paper, and then the characteristic parameters are analyzed. Uniform formulas for the slip ratio calculated from one and two dimension scales have been proved. In this way, the contact areas obtained from the experiments are larger than the calculation results for the normal impact models.

It is concluded that the characteristic parameters of the contact surface can be divided into three phases: nearly flat, decrease and bifurcation phases with the impact angle increasing. The forward spin can make geometrical sizes increase compared with the no initial spin case, but it has an opposite effect for the backward spin. When the sphere impacts with a rubber cushion, the results with different initial spins are approximately equal to or greater than the no initial spin case. The slip ratio corresponds to the three phases of slow increase, flat and sharp increase. The change trend of the first two is consistent with the impulse ratio presented in the literature. The effects of initial spin on the motion state depend on the parameters of the tangential velocity and force at the interface. This is different from the viewpoint expressed by Dong and Moys who claimed that the forward spin just promoted sliding, while the backward spin hindered sliding.

Acknowledgements

This research is jointly funded by the China Postdoctoral Science Foundation (No. 204225); Educational Committee of Henan Province of China (No. 20B210010); Commission of Science Technology of Henan Province of China (No. 202102110127); and Henan Agricultural University (No. 30500461).

References

1. ARYAEI A., HASHEMNIA K., JAFARPUR K., 2010, Experimental and numerical study of ball size effect on restitution coefficient in low velocity impacts, *International Journal of Impact Engineering*, **37**, 1037-1044
2. BRACH R.M., 1984, Friction, restitution, and energy loss in planar collisions, *Journal of Applied Mechanics*, **51**, 164-170
3. CHEHAIBI K., MRAD C., NASRI R., 2019, Collision modeling of single unit impact absorber for mechanical systems vibration attenuation, *Journal of Theoretical and Applied Mechanics*, **57**, 947-956
4. CROSS R., 2019, Oblique impact of a steel ball, *Powder Technology*, **351**, 282-290
5. DOMÉNECH-CARBÓ A., 2021, Independent friction-restitution approach to analyze anomalies in normal kinematic restitution in oblique impact, *Mechanics Research Communications*, **113**, 103699
6. DI RENZO A., DI MAIO F.P., 2004, Comparison of contact-force models for the simulation of collisions in DEM-based granular flow codes, *Chemical Engineering Science*, **59**, 3, 525-541
7. DONG H., MOYS M.H., 2006, Experimental study of oblique impacts with initial spin, *Powder Technology*, **161**, 22-31
8. FOERSTER S.F., LOUGE M.Y., CHANG H., ALLIA K., 1994, Measurements of the collision properties of small spheres, *Physics of Fluids*, **6**, 1108-1115

9. FU H., KARKEE M., HE L., DUAN J., LI J., ZHANG Q., 2020, Bruise patterns of fresh market apples caused by fruit-to-fruit impact, *Agronomy*, **10**, 59
10. GAO W., WANG J., YIN S., FENG Y.T., 2019, A coupled 3D isogeometric and discrete element approach for modelling interactions between structures and granular matters, *Computer Methods in Applied Mechanics and Engineering*, **354**, 441-463
11. GORHAM D.A., KHARAZ A.H., 2000, The measurement of particle rebound characteristics, *Powder Technology*, **112**, 193-202
12. HASHEMNIA K., ASKARI O., 2019, Experimental and finite element analysis of oblique impacts with different initial spins, *Mechanics Research Communications*, **99**, 68-72
13. KHARAZ A.H., GORHAM D.A., SALMAN A.D., 2001, An experimental study of the elastic rebound of spheres, *Powder Technology*, **120**, 281-291
14. KOMARNICKI P., STOPA R., KUTA Ł., SZYJEWICZ D., 2017, Determination of apple bruise resistance based on the surface pressure and contact area measurements under impact loads, *Computers and Electronics in Agriculture*, **142**, 155-164
15. LORENZ A., TUOZZOLO C., LOUGE M.Y., 1997, Measurement of impact properties of small, nearly spherical particles, *Experimental Mechanics*, **37**, 292-298
16. MAW N., BARBER J.R., FAWCETT J.N., 1977, The rebound of elastic bodies in oblique impact, *Mechanics Research Communications*, **4**, 17-22
17. MORENO R., GHADIRI M., ANTONY S.J., 2003, Effect of the impact angle on the breakage of agglomerates: a numerical study using DEM, *Powder Technology*, **130**, 132-137
18. MUELLER P., ANTONYUK S., STASIAK M., TOMAS J., HEINRICH S., 2011, The normal and oblique impact of three types of wet granules, *Granular Matter*, **13**, 455-463
19. MÜLLER P., PÖSCHEL T., 2012, Oblique impact of frictionless spheres: on the limitations of hard sphere models for granular dynamics, *Granular Matter*, **14**, 115-120
20. STRONGE W.J., JAMES R., RAVANI B., 2001, Oblique impact with friction and tangential compliance, *Philosophical Transactions of the Royal Society A*, **359**, 2447-2465
21. TAKIZAWA S., YAMAGUCHI R., KATSURAGI H., 2020, A novel experimental setup for an oblique impact onto an inclined granular layer, *Review of Scientific Instruments*, **91**, 014501
22. THORNTON C., NING Z., 1998, A theoretical model for the stick/bounce behaviour of adhesive, elastic-plastic spheres, *Powder Technology*, **99**, 154-162
23. WALTON O.R., 1993, Numerical simulation of inelastic, frictional particle-particle interactions, [In:] *Particulate Two-Phase Flow*, Rocco M.C. (Edit.), 884-911
24. WU C.Y., THORNTON C., LI L.Y., 2003, Coefficients of restitution for elastoplastic oblique impacts, *Advanced Powder Technology*, **14**, 435-448
25. YE X.Y., WANG D.M., ZHANG X.Y., ZHANG C.F., DU W., SU X., LI G., 2021, Projectile oblique impact on granular media: penetration depth and dynamic process, *Granular Matter*, **23**, 48